Fully Differential 5-GHz LC-Tank VCOs with Improved Phase Noise and Wide Tuning Range

Ja-Yol Lee, Chan Woo Park, Sang-Heung Lee,
Jin-Young Kang, and Seung-Hyeub Oh

In this paper, we propose two LC voltage-controlled oscillators (VCOs) that improve both phase noise and tuning range. With both $1/f$ induced low-frequency noise and low-frequency thermal noise around DC or around harmonics suppressed significantly by the employment of a current-current negative feedback (CCNF) loop, the phase noise in the CCNF LC VCO has been improved by about 10 dB at 6 MHz offset compared to the conventional LC VCO. The phase noise of the CCNF VCO was measured as -112 dBc/Hz at 6 MHz offset from 5.5 GHz carrier frequency. Also, we present a bandwidth-enhanced LC VCO whose tuning range has been increased about 250 % by connecting the varactor to the bases of the cross-coupled pair. The phase noise of the bandwidth-enhanced LC-tank VCO has been improved by about 6 dB at 6 MHz offset compared to the conventional LC VCO. The phase noise reduction has been achieved because the DC-decoupling capacitor Cc prevents the output common-mode level from modulating the varactor bias point, and the signal power increases in the LC-tank resonator. The bandwidth-enhanced LC VCO represents a 12 % bandwidth and phase noise of -108 dBc/Hz at 6 MHz offset.

Keywords: VCO, phase noise, CCNF, flicker noise, LC-tank.

Manuscript received Feb. 3, 2005; revised Aug. 16, 2005.
The material in this work was presented in part at IT-SoC 2004, Seoul, Korea, Oct. 2004.
Ja-Yol Lee (phone: +82 42 860 5929, email: ljylna@etri.re.kr), Sang-Heung Lee (email: shlee@etri.re.kr), and Jin-Young Kang (email: jykang@etri.re.kr) are with Basic Research Laboratory, ETRI, Daejeon, Korea.
Chan Woo Park (email: chanwoo@etri.re.kr) is with Future Technology Research Division, ETRI, Daejeon, Korea.
Seung-Hyeub Oh (email: ohseung@chungnam.ac.kr) is with the Department of Electronics Engineering, Chungnam National University, Daejeon, Korea.

I. Introduction

As a voltage-controlled oscillator (VCO) with high purity is necessary for satisfying the stringent phase noise requirement in wireless communication systems such as CDMA and Global System for Mobile Communications (GSM), many techniques to reduce the phase noise of the local oscillator have been proposed [1] - [7].

The low phase noise of a carbon-doped InGaP heterojunction bipolar transistor (HBT) oscillator has been achieved by both a buffering resistive collector circuit with a tuning diode and a resonating emitter circuit with a micro-strip line [2].

In a differential LC-tank VCO, various noise sources come from the cross-coupled pair, tail current source, and lossy LC-tank resonator. Of all the noise sources, low-frequency noise such as flicker noise mainly contributes to phase noise. For the purpose of removing both the thermal noise around the even harmonics and the low-frequency noise from the tail current source that is upconverted to around the carrier, both the LC noise filter and inductive degeneration are utilized on the tail current source [4]. In a field-effect transistor (FET) oscillator, the low-frequency feedback can diminish the induced input noise voltage of the oscillating FET due to the low-frequency noise such as flicker noise at the gate node, bringing down the interaction between the oscillating FET and the flicker noise source. Therefore, phase noise may be reduced using a well-designed low-frequency feedback network that consists of a resistor and feedback amplifier [5], [6].

Also, the dual-conversion receiver with a baseband dual-path architecture has been proposed to resolve flicker noise and DC offset [7]. It has been reported that a strained SiGe pMOSFET

is suitable for a low phase noise VCO design due to its low $1/f$ noise characteristics [8].

In recent years, wideband and low phase noise LC-tank VCOs have been developed for multi-band multi-mode transceivers to give different communication services to users. Among RF components, it is difficult to design a wideband and low phase noise LC-tank VCO without using additional complex circuits or special varactors [9], [10]. For the purpose of achieving the wideband and low phase noise LC-tank VCO, a different band switching has been presented. This band switching is implemented by digitally controlling the MOS capacitors. But this method makes the phase-locked loop system complex [9]. Also, Neric [10] proposed the differentially tunable accumulation-mode MOS (AMOS) varactor in order to obtain wideband and low noise VCO characteristics. Using the AMOS varactor fabricated on a silicon-on-insulator (SOI), the tuning range of the VCO was over 50 %. Additionally, the differential tuning method prevents phase noise degradation due to the high VCO sensitivity.

In this paper, we propose two LC-tank VCO topologies to lower the phase noise of the conventional LC-tank VCO. One of the two proposed LC-tank VCOs is termed the current-current negative feedback (CCNF) VCO. The phase noise of this CCNF VCO is improved by using the low-frequency CCNF loop. The proposed CCNF LC-tank VCO represents about a 10 dB reduction of phase noise compared to the conventional LC-tank VCO.

The other is the bandwidth-enhanced and phase noise-improved LC-tank VCO. In order to achieve a wide tuning range, we utilize a method to widen the effective negative resistance range of the cross-coupled pair through the proposed wideband LC-tank VCO. Also, the DC-decoupling capacitor or feedback capacitor C_c of the proposed wideband LC-tank VCO prevents the modulated output common mode from injecting into the varactor and fluctuating the varactor bias point due to the low-frequency noise. This prevention of the common-mode modulation (CMM) to frequency modulation (FM) conversion avoids phase noise corruption. The proposed wideband LC-tank VCO represents about a 250 % increment of tuning range and about a 6 dB reduction of phase noise compared to the conventional LC-tank VCO.

This paper is organized as follows. Section II briefly depicts the reported low-frequency noise upconversion to phase noise in the conventional differential LC-tank VCO. Section III describes the proposed CCNF LC-tank VCO in detail. In section IV, we mention the effective negative resistance and present a simple method to widen the tuning range through the position change of the varactor. Finally, conclusions are given in section V.

II. Flicker Noise Upconversion in the Conventional LC-Tank VCO

All low-frequency noise such as flicker noise is generated at the bases of the cross-coupled transistors and the tail current source as shown in the conventional LC-tank VCO of Fig. 1. The low-frequency variation of tail bias current I_E due to flicker noise V_{nf} results in the fluctuated ΔI_E. Due to the fluctuation of I_E, the amplitude of oscillation frequency is varied, and this modulation is termed AM. Then, the AM noise V_{am} of Fig. 1 modulates oscillation frequency by varying the average varactor capacitance, and this modulation of frequency induces phase noise [11], [12]. Also, the low-frequency fluctuation of the tail current I_E modulates the output common-mode level V_{cm} by ΔV_{cm} as shown in Fig. 1. This modulated common-mode level shakes the varactor bias point and causes phase noise [13]-[15].

As another noise, the thermal noise of tail current source I_{ntail} exists around the second harmonic of the oscillation frequency. The high-frequency thermal noise is down-converted to phase noise by the mixing operation of the cross-coupled switching transistors. Also, this thermal noise exists around all even

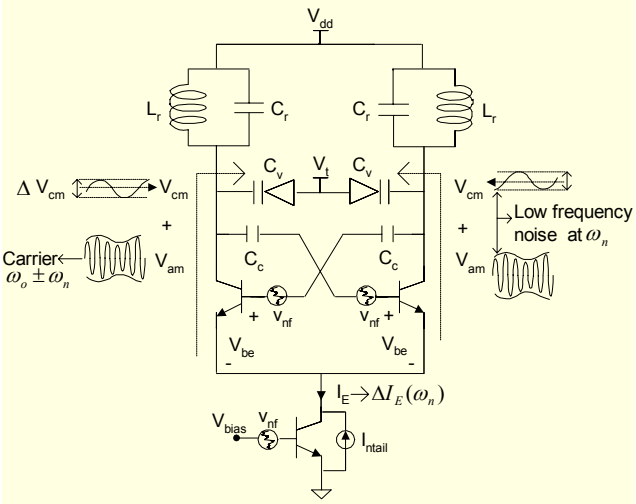

Fig. 1. Flicker noise modulation of the output common mode and the carrier amplitude in the conventional LC-tank differential VCO.

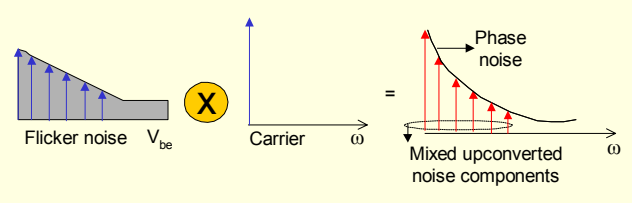

Fig. 2. Mixed noise components between V_{be} and the carrier contribute to phase noise around the carrier frequency.

harmonics of which the thermal noise around the second harmonic dominantly contributes to phase noise [5], [15].

Figure 2 represents the phase noise mechanism induced by mixing the carrier and V_{be} of the switch transistors of Fig. 1 through the nonlinear operation of the switch transistors. Here, V_{be} represents the spectrum of the flicker noise induced voltage, and the flicker noise V_{nf} exists at the base of the switch transistors as shown in Fig. 1. The mixed noise spectra of Fig. 2 represent the up-converted AM noise sidebands around the carrier frequency. Finally, the up-converted AM noise sidebands are translated into phase noise through the phase modulation of the LC-tank resonator.

Figure 3 shows the complete circuit diagram of the 5.5 GHz conventional LC-tank differential VCO. In Fig. 3, the thermal noise around the second harmonic of the oscillation frequency is shunted to ground by connecting capacitor C_p between the collector node of the tail current source and ground. The C_p of 10 pF is used for filtering out the thermal noise to ground. The DC-decoupling capacitor C_c has a role to block the DC flow and couple the RF signal power. Also, C_c prevents the forward bias of the base-collector junction of the switch transistor, and this action results in high signal amplitude in the LC-tank resonator, lowering phase noise. The LC-tank VCO core is buffered by the CC-CE pair that represents high input and output impedance.

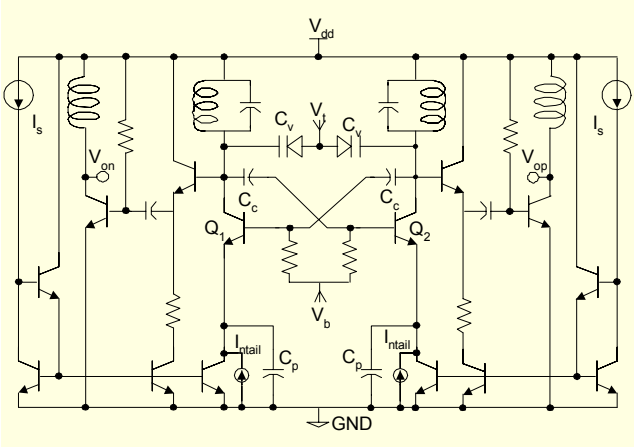

Fig. 3. Complete circuit diagram of the conventional LC-tank VCO.

III. Proposed CCNF LC-Tank VCO

1. Intuitive Depiction of the CCNF LC-Tank VCO

In this section, we qualitatively describe the effect of the CCNF loop to the low-frequency noise suppression. Figure 4 represents the differential LC-tank VCO with CCNF loop. The CCNF LC-tank VCO of Fig. 4 is a Colpitts-type oscillator because the positive feedback is generated by the base-emitter capacitance (C_{be1}) of Q_1 and feedback capacitor C_p, and hence oscillation is induced by the positive feedback. The left-side CCNF LC-tank VCO consists of an oscillating amplifier Q_1, a low-frequency feedback resistor R_f, a high-frequency feedback capacitor C_p, and a feedback amplifier Q_2. The two identical CCNF LC-tank VCOs are symmetrically connected to each other through the LC-tank resonator for taking the differential output. In the proposed CCNF LC-tank VCO of Fig. 4, the low-frequency emitter current of Q_1 is sampled by R_f, and then is injected into the base of Q_2. For this reason, the feedback mechanism is called a current-current negative feedback. Looking at the CCNF loop, the low-frequency noise induced by flicker noise V_{nf} is sampled by R_f, and is then negatively fed back to the base of Q_1 through Q_2. Then, the negatively fed back low-frequency noise component cancels the flicker noise induced low-frequency noise voltage at the base port of Q_1. Accordingly, the low-frequency noise of transistor Q_1 is suppressed by the CCNF loop. Also, the low-frequency noise from the tail current is attenuated by R_f, and the high-frequency thermal noise around the second harmonic of oscillation from the tail current is more or less filtered out to ground by C_p. The feedback amplifier Q_2 of Fig. 4 has a role to amplify the sampled low-frequency noise voltage.

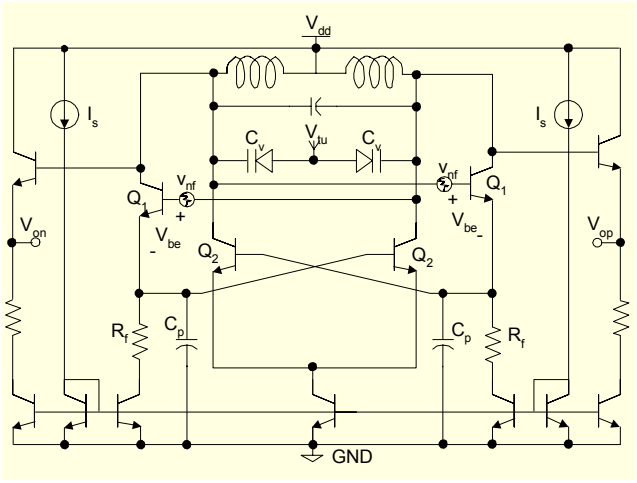

Fig. 4. Complete circuit diagram of the CCNF LC-tank VCO.

2. Low-Frequency Analysis of the CCNF LC-Tank VCO

Figure 5 shows a low-frequency equivalent circuit of the proposed CCNF LC-tank VCO. The low-frequency equivalent circuit of Q_2 is simply drawn in the dashed line of Fig. 5. Here, r_b represents both the base spreading resistance and contact resistance of Q_2, and r_π represents the incremental resistance of the forward biased base-emitter diode of the same. The mixed noise components of the flicker noise induced voltage V_{be} and carrier voltage are up-converted to sidebands around the carrier

by the nonlinear mixing operation of the oscillating amplifier Q_1, and hence the up-converted sideband noises do significantly degrade phase noise. According to [5] and [6], if V_{be} is to be reduced by a negative feedback loop, the up-converted noise components of Fig. 2, due to the mixing operation of the nonlinear device Q_1, are in some degree lessened, and hence phase noise can be reduced. Accordingly, V_{be} can be reduced by the proposed CCNF loop through the low-frequency equivalent circuit in Fig. 5. At first, V_{be} is reduced by the locally negative feedback through R_f as given by

$$V_{be} = \frac{v_{nf}}{1 + A_{v1}}, \tag{1}$$

where A_{v1} is the voltage gain of emitter follower Q_1, whose gain is 1. Secondly, considering the CCNF negative feedback loop including the local negative feedback by R_f, V_{be} is much more suppressed as given by

$$V_{be} = \frac{v_{nf}}{1 + A_{v1} + A_{v1}A_{v2}\dfrac{r_\pi}{r_b + r_\pi}}, \tag{2}$$

where A_{v2} is the voltage gain of Q_2. As expressed by (1) and (2), it is proven that V_{be} can be reduced by the local negative feedback due to R_f and the proposed CCNF loop. By (2), as A_{v2} increases, V_{be} becomes smaller, and the up-converted sideband noise components become much more lessened. Therefore, phase noise degradation due to the up-conversion of flicker noise V_{nf} at the base of the nonlinear amplifier Q_1 can be completely removed.

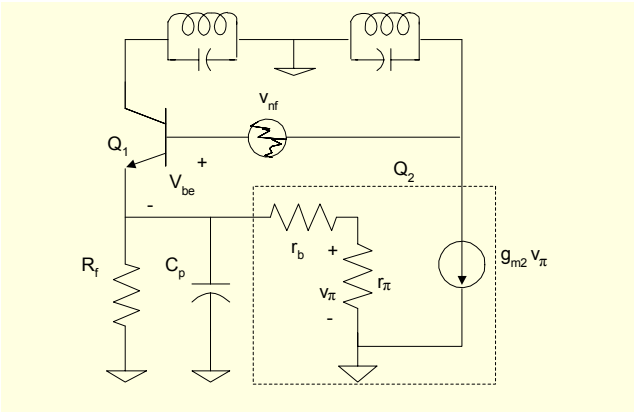

Fig. 5. Low-frequency equivalent circuit of the CCNF LC-tank VCO.

3. Input Impedance of the CCNF LC-Tank VCO

Figure 6 shows the simplified high-frequency equivalent circuit for calculating the input impedance of the CCNF LC-tank VCO. The small-signal equivalent circuit of Fig. 6 represents only the active part to generate negative resistance except for the LC-tank resonator. Here, all low-frequency resistors are ignored because the input impedance is calculated at high frequency. Also, the miller capacitances of Q_1 and Q_2 are considered only at the input port of each transistor, and are neglected at the output port because the miller effect is usually small there. If applying test signal V_s and measuring I_s, the calculated input impedance is given by

$$\begin{aligned} Z_{in} &= \frac{g_{m1} + j\omega(C_{be1} + C_{be2} + C_p)}{g_{m1}g_{m2} - \omega^2 C_{be1}(C_{be2} + C_p)} \\ &\cong -\frac{g_{m1}}{\omega^2 C_{be1}(C_{be2} + C_p)} - j\frac{C_{be1} + C_{be2} + C_p}{\omega C_{be1}(C_{be2} + C_p)}, \end{aligned} \tag{3}$$

where g_{m1} and g_{m2} are the transconductances of Q_1 and Q_2, respectively, and C_{be1} and C_{be2} are base-emitter capacitances including a miller effect of Q_1 and Q_2, respectively. Here, it is assumed that $g_{m1}g_{m2} << \omega^2 C_{be1}(C_{be2} + C_p)$ at high frequency. From (3), it is well known that the input impedance of the CCNF LC-tank VCO is similar to the input impedance of the Colpitts oscillator. Accordingly, it is proven that the CCNF LC-tank VCO is a Colpitts-type oscillator as argued in section III.1.

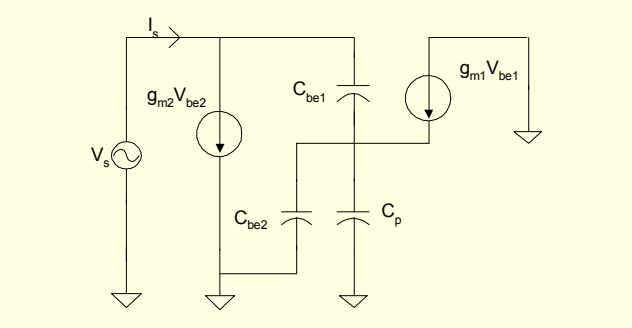

Fig. 6. High-frequency equivalent circuit of the CCNF LC-tank VCO.

Figure 7 represents the simulated input resistance of the high-frequency equivalent circuit of the CCNF LC-tank VCO. As frequency increases, the negative resistance reaches a minimum point, and then sharply rises as shown in Fig. 7. That is, if the value of C_p is 1 pF, the negative resistance decreases due to the small-valued denominator $[g_{m1}g_{m2}-\omega^2 C_{be1}(C_{be2} + C_p)]$ at a frequency below 5 GHz, but rapidly rises due to the neglect of $g_{m1}g_{m2}$ of (3) at a frequency above 5 GHz. From (3) and Fig. 7, it turns out that the magnitude of the negative resistance becomes much larger as C_p decreases. Also, the maximum negative resistance point concentrates upon the 5 GHz band, which is the frequency band suited to our target. Accordingly, the high oscillation signal power can be achieved

under a given bias condition. Here, a C_p of 2 pF is used in the CCNF LC-tank VCO.

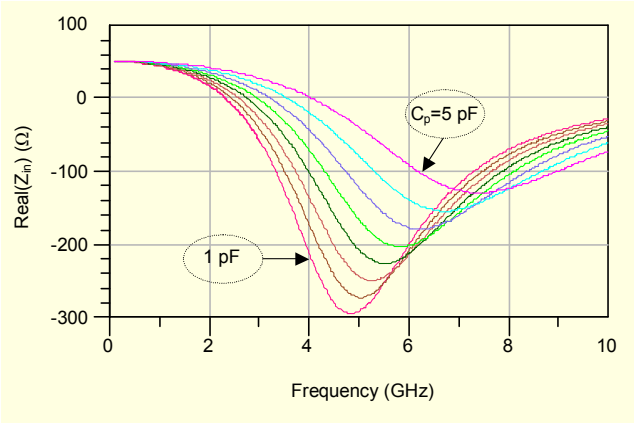

Fig. 7. Simulated input resistance of the CCNF LC-tank VCO.

4. Measurement of Phase Noise

For this section, we fabricated both the conventional LC-tank VCO of Fig. 3 and the CCNF LC-tank VCO of Fig. 4 for the purpose of comparing their phase noises. Both the conventional LC-tank VCO and the CCNF LC-tank VCO were manufactured using 0.8-μm SiGe HBT process technology, and their chip sizes are 1.0 mm × 0.8 mm and 0.8 mm × 0.7 mm, respectively, as shown in Fig. 18.

Figure 8 represents a phase noise comparison between the conventional LC-tank VCO and the CCNF LC-tank VCO. The phase noise of the conventional LC-tank VCO is -102 dBc/Hz at 6 MHz offset, while the phase noise of the CCNF LC-tank VCO represents -112 dBc/Hz at 6 MHz offset from 5.42 GHz carrier frequency. From the compared graph of Fig. 8, the phase noise of the CCNF LC-tank VCO has been reduced by about 10 dB compared to the conventional LC-tank VCO. Accordingly, it turns out that the low-frequency noise from the tail current and the switch transistor are suppressed by the proposed CCNF loop, and the high-frequency thermal noise around the second harmonic is more or less kept down by both R_f and C_p. The tuning range of the CCNF LC-tank VCO is measured from 5410 to 5540 MHz as shown in Fig. 15, and the high-order harmonics of the CCNF LC-tank VCO are suppressed by about -27 dBc. This result is not shown here due to space constraints.

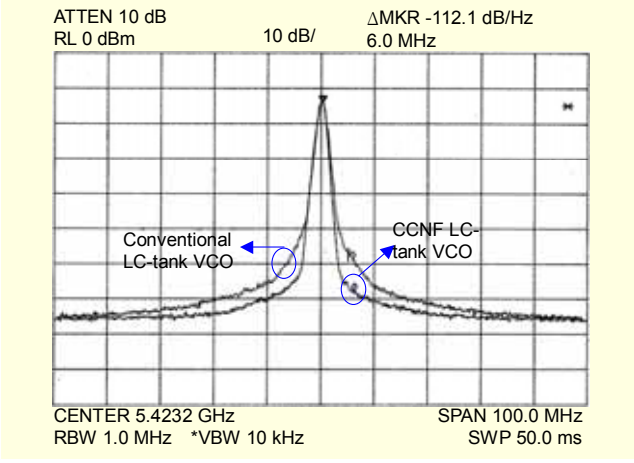

Fig. 8. Measured phase noise comparison between the conventional LC-tank VCO and CCNF LC-tank VCO.

IV. Bandwidth-Enhanced LC-Tank VCO

1. Frequency Tuning Range Enhancement

For the purpose of widening the tuning range of the conventional LC-tank VCO of Fig. 3, a technique is described in this section. For a wideband VCO, broad negative resistance as well as a maximum varactor capacitance ratio is required. For improving the tuning range of a VCO, an SOI AMOS varactor was used in [10]. However, the method used in their approach doesn't consider the negative resistance range of a VCO at all. Accordingly, we are to widen the effective negative resistance range using the proposed wideband LC-tank VCO of Fig. 9 for a much wider tuning range. The proposed wideband LC-tank VCO of Fig. 9 is a modified VCO topology of the conventional LC-tank VCO by connecting the varactor to the base of the switch transistor. If C_c is short, the cross-coupled pairs of the two VCOs are identical.

In general, the loss of an LC-tank resonator also increases as frequency increases. Therefore, the negative resistance must

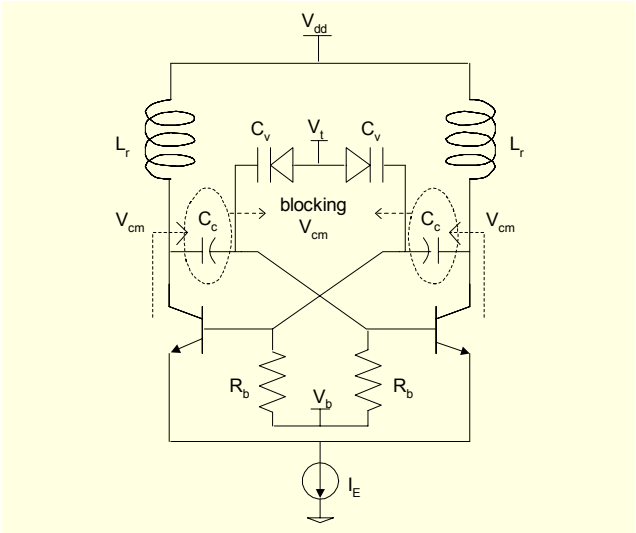

Fig. 9. Proposed wideband LC-tank VCO.

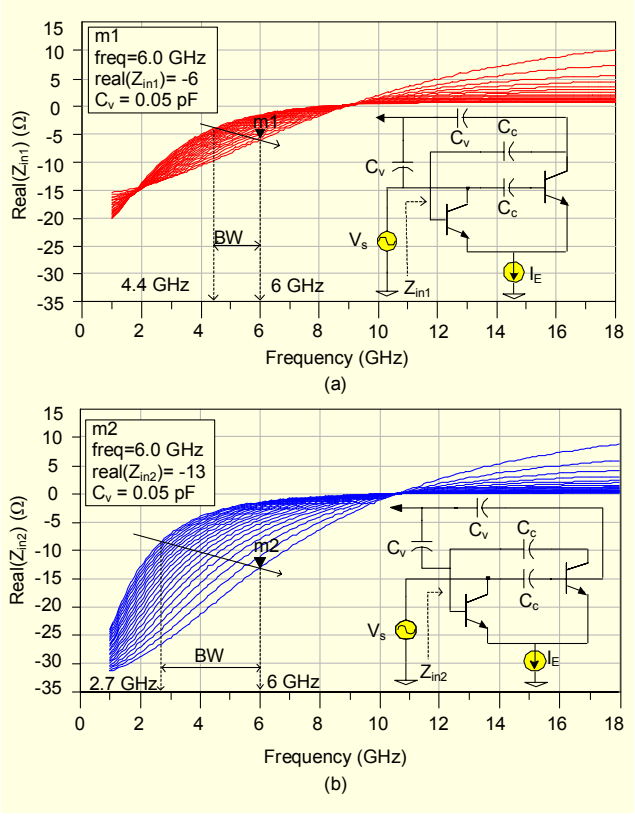

Fig. 10. (a) Effective negative resistance range of the conventional LC-tank VCO, and (b) effective negative resistance range of the proposed wideband LC-tank VCO.

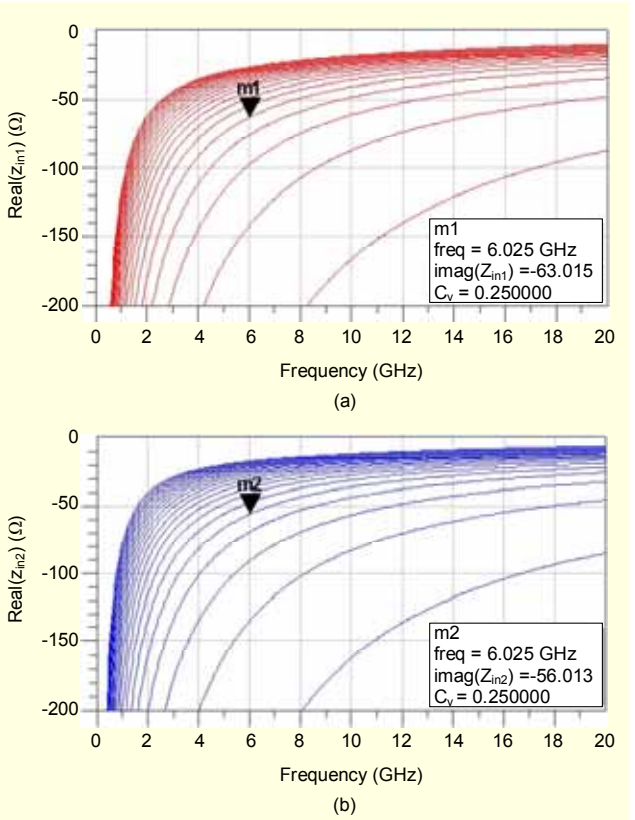

Fig. 11. Simulated imaginary part of the input impedance of (a) a conventional LC-tank VCO, and of (b) the proposed wideband LC-tank VCO.

also increase in order to compensate for the increasing loss resistance of the LC-tank, and hence to achieve oscillation at a higher frequency. In fact, as the value of the varactor capacitor C_v decreases, that is, oscillation frequency $f_o=1/(L_r \cdot C_v)^{1/2}$ increases, the input negative resistance of the cross-coupled pair must increase at a high frequency as argued just before. From the simulation result of Fig. 10, using each circuit configuration in the simulation windows, the magnitude of input negative resistance increases as the value of C_v is arbitrarily changed from 1.05 to 0.05 pF. In Fig. 10, the arrow body marked by m1 or m2 indicates the moving negative resistance points at which oscillation is caused. BW of Fig. 10 represents the effective negative resistance range, and if deviating from BW, oscillation cannot be generated.

Figure 10(a) represents the simulated negative resistance of the conventional LC-tank VCO of Fig. 3. In Fig. 10(a), the effective negative resistance range is simulated from 4.4 to 6 GHz, and hence BW is 1.6 GHz. Figure 10(b) shows the simulated negative resistance range of the proposed wideband LC-tank VCO. From Fig. 10(b), the effective negative resistance range is simulated from 2.7 to 6 GHz. The BW of the proposed wideband LC-tank VCO is much wider than the conventional 3.3 GHz. Figure 11 represents the simulation results on the imaginary part of the input impedance of two VCOs. Both imaginary parts versus C_v do almost vary equivalently as shown in Fig. 11. This result can be derived from the fact that both imaginary parts of (4) and (5) represent a similar variation depending on the value of C_v. From the above results, therefore, the proposed wideband LC-tank VCO can achieve a much wider tuning range than the conventional LC-tank VCO due to a much wider BW. Also, the magnitude of the negative resistance of the proposed wideband LC-tank VCO is much larger than the conventional LC-tank VCO as represented by Fig. 10 and (5).

$$Z_{in1} = -\frac{2g_m C_c (C_c - 2C_v)}{g_m^2 (C_c - 2C_v)^2 + 4\omega^2 C_c^2 C_v^2} - j\frac{4\omega C_c C_v}{g_m^2 (C_c - 2C_v) + 4\omega^2 C_c C_v^2}, \quad (4)$$

$$Z_{in2} = -\frac{2g_m (C_c + C_v)}{C_c (g_m^2 + 4\omega^2 C_v^2)} - j\frac{4\omega (C_c + C_v) C_v}{C_c (g_m^2 + 4\omega^2 C_v^2)}, \quad (5)$$

where g_m is the transconductance of the switch transistor, and

C_c is the DC-decoupling capacitor. From (4) and (5), it turns out that the BW of the conventional LC-tank VCO narrows due to the subtracting term (C_c-2C_v) of (4), while the BW of the wideband LC-tank VCO widens due to the adding term (C_c+C_v) of (5). Also, if C_c>>C_v, (4) and (5) become identical as given by

$$Z_{in1} = Z_{in2} = -\frac{2g_m}{g_m^2 + 4\omega^2 C_v^2} - j\frac{4\omega C_v}{g_m^2 + 4\omega^2 C_v^2}. \quad (6)$$

That is, it is proven through (6) that if C_c has a large value, the cross-coupled pairs of the conventional LC-tank VCO and the wideband LC-tank VCO are identical, as previously argued.

Figure 12 shows the simulated tuning ranges of the conventional LC-tank VCO of Fig. 3 and the proposed wideband LC-tank VCO of Fig. 13 when varactors are biased from 0 to 2.5 V. Here, the extracted value of the varactor at 5 GHz is varied from 260 to 400 fF, and its Q-factor is varied from 32 to 27. As shown in Fig. 12, the conventional LC-tank VCO shows a tuning range of 450 MHz, while the proposed wideband LC-tank VCO represents a much wider tuning range of 1 GHz. Accordingly, it is proven from the simulation results that the tuning range of the proposed wideband LC-tank VCO increases by about two times that of the conventional LC-tank VCO.

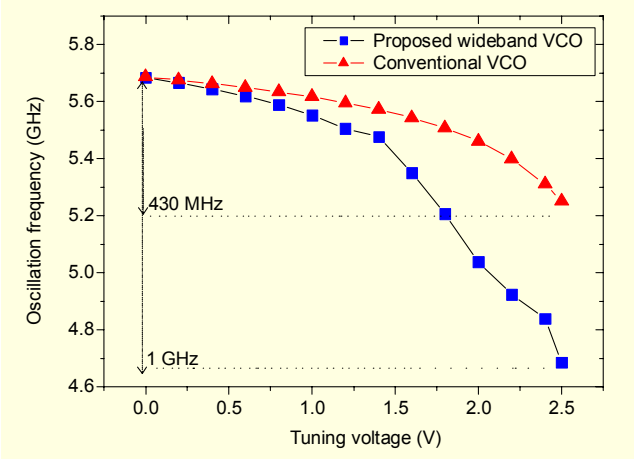

Fig. 12. Simulated tuning ranges of the conventional LC-tank VCO and the proposed wideband LC-tank VCO.

2. Phase Noise Reduction by Modulated Common-Mode Level Rejection and High Signal Swing at the Resonator

All low-frequency noise is generated at the cross-coupled pair and tail current source as explained in Fig. 1 of section II. As represented in Fig. 1, the low-frequency modulation of the output common-mode level V_{cm} fluctuates the varactor bias point by ΔV_{cm}, causes a frequency jitter, and hence induces phase noise. The total varactor bias voltage V_{con} is given by

$$V_{con} = V_t - V_{cm} = V_t - [V_{dd} - \alpha_f (I_E + \Delta I_E) r_p], \quad (7)$$

where ΔI_E represents the low-frequency modulation of I_E, r_p is a parasitic resistor of the LC-tank, and α_f is common-base forward short-circuit current gain. Equation (7) shows that the low-frequency variation of I_E modulates V_{cm}, and then V_{con} [15]. This variation of V_{con} modulates varactor capacitance C_v, and hence oscillation frequency as expressed by

$$C_v = C_o + K_{vco} V_{con}, \quad (8)$$

$$f_o = \frac{1}{\sqrt{L_r (C_r + C_v)}}, \quad (9)$$

where C_o is the zero bias varactor capacitance, K_{vco} is the sensitivity of VCO in Hz/V, f_o is a carrier frequency, and L_r and C_r are the inductance and capacitance of the LC-tank, respectively. Accordingly, the modulation of the common-mode level V_{cm} to the varactor bias V_t is prevented by the DC-decoupling capacitor C_c in the proposed wideband LC-tank VCO of Fig. 9 because V_{cm} is blocked by C_c independent of the low-frequency modulation of V_{cm}, and hence the phase noise degradation is more or less alleviated. However, the varactor of Fig. 9 does somewhat suffer from common-mode variation without using the bandgap reference circuit for biasing the base of the cross-coupled transistor. But this base common-mode variation by low-frequency noise can be ignored, compared with the output common-mode variation at the collector node.

The proposed wideband LC-tank VCO of Fig. 9 shows that there is more room for phase noise improvement. This can be achieved by increasing oscillation signal power in the LC-tank resonator by maximizing the signal swing at the collector node

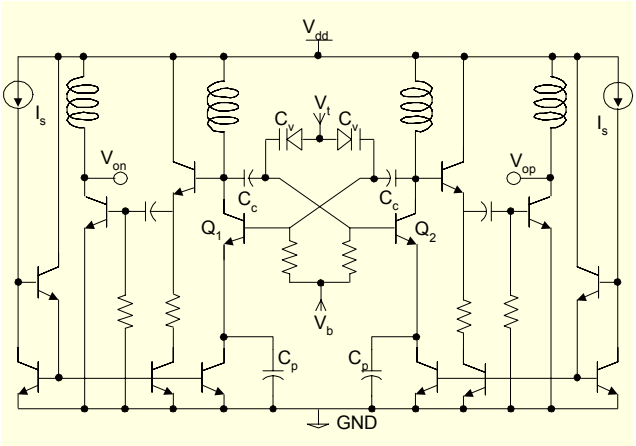

Fig. 13. Complete circuit diagram of the proposed wideband LC-tank VCO of Fig. 9.

of the switch transistor. That is, the prevention of forward bias of the collector-base (CB) junction of the switch transistor is to maximize the oscillation signal swing. The capacitance divider, consisting of C_v and C_c, does just prevent the CB junction from being forward-biased in the proposed wideband LC-tank VCO of Fig. 9. A complete schematic of the proposed wideband LC-tank VCO is shown in Fig. 13. Like the conventional LC-tank VCO of Fig. 3, C_p of 10 pF is used to attenuate the thermal noise of the tail current, and the CC-CE amplifier drives the 50 Ω load.

3. Measurement of Tuning Range and Phase Noise

In this section, we fabricated the proposed wideband LC-tank VCO of Fig. 13 using 0.8 μm SiGe HBT technology. A chip photograph of the wideband LC-tank VCO is shown in Fig. 18, and its size is 1.0 mm × 0.8 mm. Figures 14 and 15 represent the measured frequency tuning bandwidths and output power of the conventional LC-tank VCO and the proposed wideband LC-tank VCO using an HP8565EC spectrum analyzer.

From the measured output power and frequency tuning range of Figs. 14 and 15, the tuning bandwidth of the conventional LC-tank VCO is 136 MHz, while the tuning bandwidth of the proposed wideband LC-tank VCO represents 643 MHz. Although the measured tuning ranges of Fig. 15 are reduced as much as half, the measured tuning curves show similar characteristics with the simulated tuning curves of Fig. 12. The bandwidth of the proposed wideband LC-tank VCO has been increased by about 507 MHz, compared to the conventional LC-tank VCO. That is, the tuning range of the proposed wideband LC-tank VCO shows about 250 % increments. In Fig. 15, the output power of the wideband LC-tank VCO has been increased by 3 dB, compared to the conventional LC-tank VCO.

Figure 16 represents the measured phase noise of the conventional LC-tank VCO and the proposed wideband LC-tank VCO. The proposed wideband LC-tank VCO represents a phase noise of -108 dBc/Hz at 6 MHz offset from 5.4 GHz. Compared with that of the conventional LC-tank VCO, the phase noise of the proposed wideband LC-tank VCO is improved by about 6 dB as shown in Fig. 16. Also, Fig. 14 shows that the RF signal power of the proposed wideband LC-tank VCO has been increased by about 3 dB, compared to the conventional LC-tank VCO. Accordingly, it is confirmed from the measured data that both the prevention of the output common-mode modulation of C_v and the increment of the RF signal power in the LC-tank resonator improve phase noise.

Figure 17 represents the phase noise of all three VCOs measured at 6 MHz offset frequency, depending on the tuning voltage. From the measured results, the phase noises of the CCNF VCO and wideband VCO have been improved by

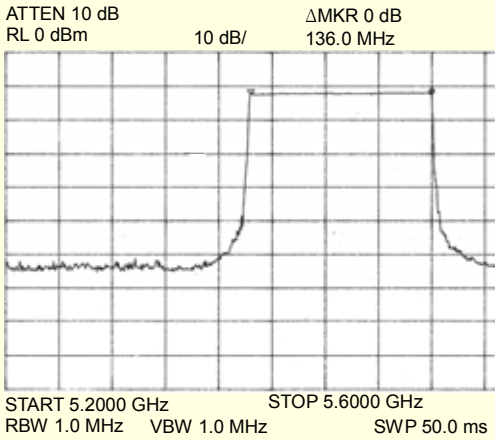

Fig. 14. Measured tuning bandwidth of (a) the conventional LC-tank VCO and (b) the proposed wideband LC-tank VCO.

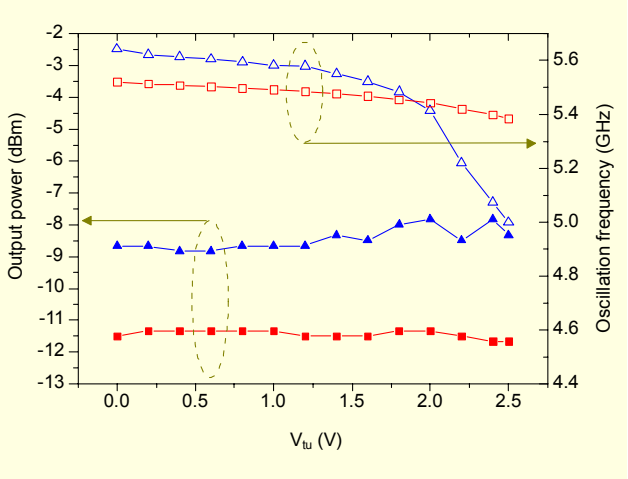

Fig. 15. Measured frequency tuning ranges and output powers of two VCOs versus tuning voltage (–△–▲–: wideband LC-tank VCO, –□–■–: conventional LC-tank VCO).

10 dB and 6 dB over entire tuning voltage, respectively. In this paper, all VCOs have been designed using a Gummel Poon BJT nonlinear model and fabricated using a 0.8-μm SiGe HBT process. But, a noise model is not included in the Gummel Poon nonlinear model. The f_t and f_{max} of the SiGe HBT are 45 GHz and 42 GHz, respectively. Manufactured chip photographs are shown in Fig. 18. The performance parameters of all VCOs are summarized in Table 1.

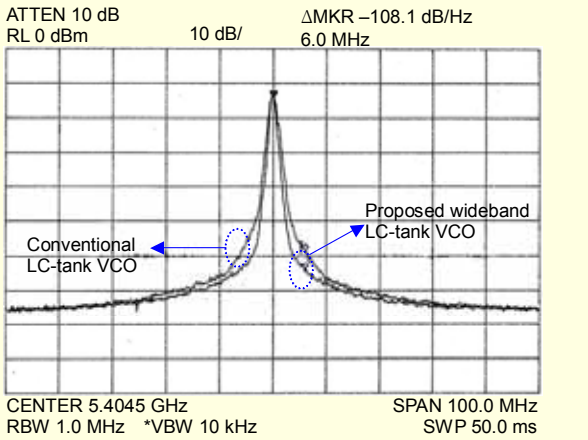

Fig. 16. Measured phase noise comparison between the conventional LC-tank VCO and the proposed wideband LC-tank VCO.

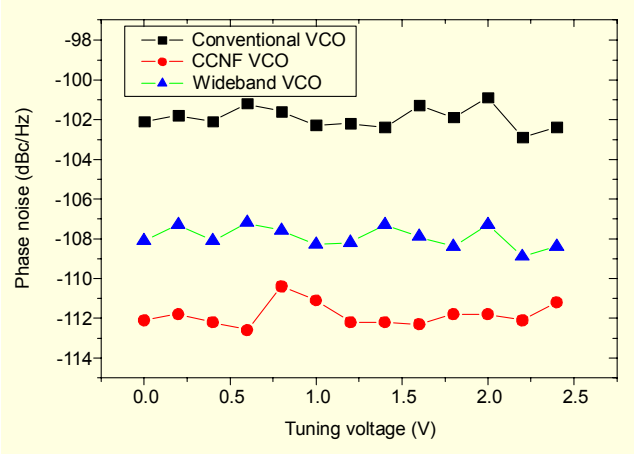

Fig. 17. Measured phase noise comparison of the fabricated VCOs versus tuning voltage.

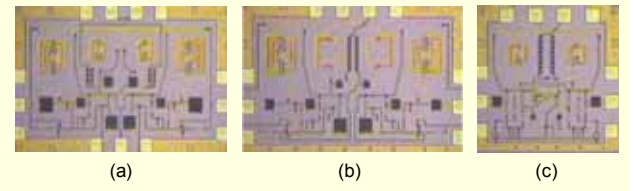

Fig. 18. Fabricated chip photographs of (a) the conventional LC-tank VCO, (b) wideband LC-tank VCO, and (c) CCNF LC-tank VCO.

Table 1. Summary of the performance parameters of the conventional VCO, CCNF VCO, and wideband VCO.

Parameter \ Type	Conventional VCO	CCNF VCO	Wideband VCO
V_d/I_{total}	2.5 V/13 mA	2.0 V/14 mA	2.5 V/13 mA
P_{out}	-11 dBm	- 12 dBm	- 8 dBm
Tuning range (MHz)	5380 - 5520	5410 - 5540	5000 - 5643
Harmonics	< -23 dBc	< -27 dBc	< -21 dBc
P.N. @6 MHz	- 102 dBc/Hz	- 112 dBc/Hz	- 108 dBc/Hz

V. Conclusions

In this paper, we have presented both the CCNF LC-tank VCO and the wideband LC-tank VCO for improving phase noise and tuning range of the conventional LC-tank VCO. Compared to the conventional LC-tank VCO, the proposed CCNF LC-tank VCO represents a phase noise reduction of about 10 dB, achieving a phase noise of -112 dBc/Hz at 6 MHz offset from 5.4 GHz carrier frequency. The phase noise improvement is attributed to both the flicker noise and thermal noise suppression from all transistors by the CCNF loop. In the proposed wideband LC-tank VCO, its tuning range has been increased by about 250% due to the widened effective negative resistance range. Also, its phase noise was reduced by about 6 dB, representing a phase noise of -108 dBc/Hz at 6 MHz offset from 5.4 GHz carrier frequency. Both the prevention of the output common-mode modulation to the varactor bias and the increment of signal power in the LC-tank resonator contribute to phase noise improvement. In conclusion, the CCNF VCO and wideband VCO proposed in this paper contribute to improve the phase noise and tuning range of a conventional LC-tank VCO.

References

[1] M. Borremans, B.De Muer, and M. Steyart., "Phase Noise Up-Conversion Reduction for Integrated CMOS VCOs," *Electron. Lett.*, vol. 36, no. 10, May 2000, pp. 857-858.

[2] Young-Gi Kim, Chang-Woo Kim, Seoung-Il Kim, Byoung-Gue Min, Jong-Min Lee, and Kyung Ho Lee, "An X-Band Carbon-Doped InGaP/GaAs Heterojunction Bipolar Transistor MMIC Oscillator," *ETRI J.*, vol. 27, no.1, Feb. 2005, pp. 75-80.

[3] B. De Muer, M. Borremans, M. Steyaert, and G. Li Puma, "A 2-GHz Low-Phase-Noise Integrated LC-VCO Set with Flicker-Noise Upconversion Minimization," *IEEE J. Solid-State Circuits,* vol. 35, no. 7, July 2000, pp. 1034 -1038.

[4] P. Andreani and H. Sjoland, "Tail Current Noise Suppression in RF CMOS VCOs," *IEEE J. Solid-State Circuits*, vol. 37, no. 3, Mar. 2002, pp. 342-348.

[5] M. Prigent and J. Obregon, "Phase Noise Reduction in FET Oscillators by Low-Frequency Loading and Feedback Circuitry Optimization," *IEEE Trans. Microwave and Theory Techn.,* vol. 35, no. 3, Mar. 1987, pp. 349-352.

[6] U.L. Rohde and F. Hagemeyer, "Feedback Technique Improves Oscillator Phase Noise," *Microwave & RF*, Nov. 1998, pp. 61-70.

[7] Seok-Bong Hyun, Geum-Young Tak, Sun-Hee Kim, Byung-Jo Kim, Jinho Ko, and Seong-Su Park, "A Dual-Mode 2.4-GHz CMOS Transceiver for High-Rate Bluetooth Systems," *ETRI J.,* vol. 26, no. 3, June 2004, pp. 229-240.

[8] Young-Joo Song, Kyu-Hwan Shim, Jin-Young Kang, and Kyung-Ik Cho, "DC and RF Characteristics of $Si_{0.8}Ge_{0.2}$ pMOSFETs: Enhanced Operation Speed and Low 1*f* Noise," *ETRI J.,* vol. 25, no. 3, June 2003, pp. 203-209.

[9] J.K. Cho, H.I. Lee, K.S. Nah, B.H. Park., "A 2-GHz Wide Band Low Phase Noise Voltage-Controlled Oscillator with On-Chip LC Tank," *IEEE Custom Integrated Circuit Conf.,* Sept. 2003, pp. 559-562.

[10] N.H.W. Fong, J.O. Plouchart, N. Zamdmer, Liu Duixian, L. Fl Wagner, C. Plett, and N.G. Tarr, "A 1-V 3.8-5.7-GHz Wide-Band VCO with Differentially Tuned Accumulation MOS Varactors for Common-Mode Noise Rejection in CMOS SOI Technology," *IEEE Trans. Microwave and Theory Techn.,* vol. 51, no. 8, Aug. 2003, pp. 1952-1959.

[11] J. Rogers, J. Macedo, and C. Plett, "The Effect of Varactor Nonlinearity on Phase Noise of Completely Integrated VCOs," *IEEE J. Solid-State Circuits,* vol. 35, no. 9, Sept. 2000, pp. 1360-1365.

[12] E. Hegazi and A.A. Abidi, "Varactor Characteristics, Oscillator Tuning Curves, and AM-FM Conversion," *IEEE J. Solid-State Circuits,* vol. 38, no. 6, June 2001, pp. 1033-1039.

[13] E. Hegazi, S. Henrink, and A.A. Abidi, "A Filtering Technique to Lower LC Oscillator Phase Noise," *IEEE J. Solid-State Circuit,* vol. 36, no. 12, Dec. 2001, pp. 1921-1930.

[14] S. Levantino, C. Samori, A. Bonfanti, S.J. Gierkink, A.L. Lacaita, and V. Boccuzzi, "Frequency Dependence on Bias Current in 5-GHz CMOS VCOs: Impact on Tuning Range and Flicker Noise Upconversion," *IEEE J. Solid-State Circuits,* vol. 37, no. 8, Aug. 2002, pp. 1003-1011.

[15] A. Ismail and A.A. Abidi, "CMOS Differential LC Oscillator with Suppressed Up-Converted Flicker Noise," *IEEE ISSCC,* Dig. Tech. Papers, 2003, pp. 98-99.

Ja-Yol Lee received the BE degree from Konkuk university, Seoul, Korea, in 1998 and the ME and PhD degrees in electronics engineering from Chungnam National University, Daejeon, in 2000 and 2005, all in electronics engineering. Since 2001, he has been with Electronics and Telecommunications Research Institute (ETRI), where he has been working as RF & Analog Circuit Designer. His research interests are PLL, RFIC and OEIC design, semiconductor device modeling, and SPICE parameter extraction and optimization. He is a member of KICS and KEES.

Chan Woo Park received the BE, MS and PhD degrees from material science and engineering from Korea Advanced Institute of Science and Technology, Daejeon, Korea, in 1994, 1996, and 2000, respectively. Since 2000, he has been with ETRI, Daejeon, Korea, as a Senior Member of Research Staff. He has been working on the development of SiGe Devices. His research interests include SiGe HBT, and IC technology, molecular electronics, and nano-electronic devices design, passive devices, and NiSi process for Nano-scale device fabrication.

Sang-Heung Lee was born in Daejeon, Korea, in 1966. He received the BE, MS, and PhD degrees in Department of Electronics Engineering from Chungnam National University, Korea, in 1988, 1992, and 1998, respectively. From 1998 to 1999, he held a position as a Post-Doctorial Researcher at ETRI in Daejeon, Korea. Since 1999, he has been working as a Circuit Design Engineer at ETRI. His current interests are RFIC and OEIC design, semiconductor device modeling, and SPICE parameter extraction and optimization.

Jin-Young Kang received the ME and PhD degrees in physics from Korea Advanced Institute of Science and Technology, in 1979 and 1991, respectively. He joined ETRI at Daejeon in 1979. He has been working on the development of SiGe Devices and Processes. At present, he is a Principal Member of Engineering Staff of SiGe Device Team at ETRI-Basic Research Laboratory.

Seung-Hyeub Oh received the BE, the MS, and the PhD degrees in Yonsei University, Seoul, Korea, in 1971, 1973 and 1982, respectively, all in electrical engineering. He worked for Tohoku University, Japan, from 1980 to 1981, as a Guest Researcher and Pennsylvania State Uninverisity, USA, from 1985 to 1986, as a Guest Researcher. Since 1984 he has been with Chungnam National University, Daejeon, Korea, where he is a Professor in the Department of Electronics Engineering. His research interests include antenna engineering and digital communication RF sub-system design. He is a member of KICS and KEES and IEEE.